Spin-asymmetric laser-driven relativistic tunneling from *p* states

Michael Klaiber and Karen Z. Hatsagortsyan
Max-Planck-Institut für Kernphysik, Saupfercheckweg 1, 69117 Heidelberg, Germany
(Received 13 October 2014; published 9 December 2014)

The tunneling ionization of an electron from a p state in a highly charged ion in the relativistic regime is investigated in a linearly polarized strong laser field. In contrast to the case of an s state, the tunneling ionization from the p state is spin asymmetric. We single out two reasons for the spin asymmetry: first, the difference of the electron energy Zeeman splitting in the bound state and during tunneling, and second, the relativistic momentum shift along the laser propagation direction during the under-the-barrier motion. Due to the latter, those states are predominantly ionized where the electron rotation is opposite to the electron relativistic shift during the under-the-barrier motion. We investigate the dependence of the ionization rate on the laser intensity for different projections of the total angular momentum and identify the intensity parameter that governs this behavior. The significant change of the ionization rate originates from the different precession dynamics of the total angular momentum in the bound state at high and low intensities.

DOI: 10.1103/PhysRevA.90.063416 PACS number(s): 32.80.Rm, 31.30.J−

I. INTRODUCTION

Recently, significant experimental effort has been invested in the investigation of relativistic regimes of strong-field ionization [1–4], which has fostered, accordingly, the development of theory [5]. In particular, specific signatures of the relativistic under-the-barrier dynamics in the photoelectron momentum distribution were pointed out recently in [6–8] and subtle spin effects in laser fields were explored in [9–15]. During the relativistic laser-atom interaction, spin effects were shown to appear in the laser-driven bound electron dynamics [16] and, in particular, in the radiation of high-order harmonics [17,18]. Spin effects arise also during tunneling ionization [19,20]. The spin effects in nonsequential double ionization of helium were considered in [21,22]. It appears that during the relativistic tunneling ionization from a ground state of a hydrogenlike ion spin asymmetry is negligible, however, the spin flip is possible when using relativistic laser intensities of the order of 10^{22} W/cm^2 and highly charged ions, with the charge state of the order of $Z \sim 30$. The question arises as to whether spin asymmetry can exist for ionization of nonspherical symmetric states.

In the nonrelativistic regime the strong-field ionization rate in the tunneling regime is calculated in the Perelomov-Popov-Terent'ev theory [23–27] for any value of the angular momentum l and the magnetic quantum number m. The laser pulse effect in the ionization of excited states of a hydrogen atom in the nonrelativistic regime is considered in [28]. The excited p state of He^+ has been proposed to control the polarization of isolated attosecond pulses [29]. In this context, the peculiarities of strong-field ionization, recollision, and high-order-harmonic generation from antisymmetric molecular orbitals are also known [30–32]. Note that the ionization from $m_l \neq 0$ states is an essential ingredient in the dynamics of multiple ionization of the atomic target in ultrastrong laser fields [33–37].

Recently, the interest in the strong-field ionization of an electron from a p state has been renewed in connection with the nonadiabatic ionization in a circularly polarized laser field [38–40]. It turns out that in the nonadiabatic regime, when the Keldysh parameter γ [41] is not small, the electron in the bound state rotating opposite to the field rotation ($m < 0$) is ionized more easily than in the corotating case. Moreover, a spin-polarization effect was found in [42] due to the interplay of the electron-core entanglement and the sensitivity of ionization in a circularly polarized field to the magnetic quantum number m_l.

In this paper we consider tunnel ionization in the relativistic regime from an exited p state of a hydrogenlike ion induced by a strong linearly polarized laser field. The main concern is to investigate the dependence of the tunneling probability on the magnetic and spin quantum numbers in the relativistic regime and to find conditions when a large spin asymmetry can exist. We will show that in the relativistic regime, even in the adiabatic case $\gamma \ll 1$, one can observe the dependence of the ionization probability on the magnetic quantum number similar to the nonrelativistic nonadiabatic regime. Those bound states are predominantly ionized where the electron rotation in the bound state is opposite to the electron relativistic shift along the propagation direction during the under-the-barrier motion.

The tunneling ionization rates from the excited p states of a hydrogenlike ion are calculated. For convenience, the relative ionization rates of the p state with respect to the s state, rather than the absolute ionization rates, are presented. For this reason we first calculate the tunneling ionization rate from the excited $2s$ state of the hydrogenlike ion. We employ a Coulomb-corrected relativistic strong-field approximation (SFA) developed in [43,44] for the description of the ionization dynamics in the relativistic regime.

II. CALCULATION OF THE IONIZATION RATE

The ionization differential rate is expressed via the transition matrix element

$$\frac{dw}{d^3\mathbf{p}} = \frac{\omega}{2\pi}|M|^2, \tag{1}$$

with the laser frequency ω. The matrix element M in the Coulomb-corrected SFA reads [44]

$$M = \int dt\, d^3\mathbf{r}\, \psi_C^V(\mathbf{r},t)\mathbf{r}\cdot\mathbf{E}(\eta)\tilde{\psi}_i(\mathbf{r},t), \tag{2}$$

where $\mathbf{E}(\eta) = \hat{\mathbf{x}}E_0\cos(\omega\eta)$ is the laser field with the phase $\eta = t - z/c$ and c is the speed of light. The final state ψ_C^V is the eikonal Coulomb-Volkov state [44], i.e., the wave function in the eikonal approximation for the electron in the continuum under the action of the laser and Coulomb fields of the atomic core. The use of the Coulomb-corrected–Volkov wave function allows us to derive quantitatively correct ionization probabilities taking into account the influence of the Coulomb field of the atomic core for the under-the-barrier dynamics. Here $\tilde{\psi}_i$ is the dressed initial bound state, which is the solution of the Schrödinger equation [44]

$$i\partial_t\tilde{\psi}_i = H_B\tilde{\psi}_i, \tag{3}$$

with the dressed bound-state Hamiltonian

$$H_B = c\boldsymbol{\alpha}\cdot\{\mathbf{p} - \hat{\mathbf{k}}[\mathbf{r}\cdot\mathbf{E}(\eta)]\} + \beta c^2 + V(\mathbf{r}), \tag{4}$$

where $\hat{\mathbf{k}}$ is the unit vector in the laser propagation direction, $V(\mathbf{r})$ is the potential of the ionic core, and $\boldsymbol{\alpha}$ and β are the Dirac matrices.

First we calculate the dressed bound states. In the case of a $2s$ state, the approximate solution of Eq. (3), taking into account only transitions between the states of the fine structure [44], is

$$\tilde{\psi}_j^{(2s)}(\mathbf{r}) = \psi_j^{(2s)}(\mathbf{r})\exp[ijA(\eta)/2c], \tag{5}$$

where $\psi_j^{(2s)}(\mathbf{r})$ is the relativistic wave function of the initial $2s$ state of the electron in the highly charged hydrogenlike ion [45]

$$\psi_j^{(2s)}(\mathbf{r}) = \left[(1-\sqrt{2I_p}r)\chi_j, i\left(\frac{I_p}{2c^2}\right)^{1/2}(2-\sqrt{2I_p}r)\frac{\boldsymbol{\sigma}\cdot\mathbf{r}}{r}\chi_j\right] \times\frac{\exp(-\sqrt{2I_p}r)(2I_p)^{3/4}}{\sqrt{\pi}}, \tag{6}$$

with the quantum number of the total angular momentum projection $j = (+,-)$, the spinors $\chi_+ = (1,0)$, $\chi_- = (0,1)$, the ionization energy I_p, and the Pauli matrices $\boldsymbol{\sigma}$ (the electron total energy in the bound state is $c^2 - I_p$ and the ionization energy I_p is related to the nuclear charge as $Z = 2\sqrt{2I_p}$). According to Eq. (5), the $2s$ state experiences a Zeeman splitting with an energy of $\varepsilon_J^{(b)} = -j\partial_t A/2c = g_S\mathbf{S}\cdot\mathbf{B}/2c$, where $S_B = \pm 1/2$, $g_S = 2$, and $A(\eta) = -E_0/\omega\sin(\omega\eta)$. Since the typical coordinate where the electron starts to leave the ion is $r \sim \sqrt{E_a/E_0}/\sqrt{2I_p}$ [44], with the atomic field strength $E_a = (2I_p)^{3/2}$ and $E_0/E_a \ll 1$ in the tunneling regime, the wave function of the initial state of Eq. (6) can be approximated

$$\psi_j^{(2s)}(\mathbf{r}) = -\left(\chi_j, i\sqrt{\frac{I_p}{2c^2}}\frac{\boldsymbol{\sigma}\cdot\mathbf{r}}{r}\chi_j\right)\frac{r\exp(-\sqrt{2I_p}r)(2I_p)^{5/4}}{\sqrt{\pi}}. \tag{7}$$

The differential ionization rate from the $2s$ state is calculated via Eqs. (1) and (2). We have evaluated the differential rate for a given p_E at the local maximum rate that is achieved at the momentum parabola [44]

$$p_k = \frac{I_p}{3c} + \frac{p_E^2}{2c}\left(1 + \frac{I_p}{3c^2}\right), \quad p_B = 0, \tag{8}$$

where p_E, p_B, and p_k are the momentum components along the laser electric field, the magnetic field, and the propagation directions, respectively. On the mentioned momentum parabola, the rate reads

$$\frac{dw_\pm^{(2s)}}{d^3\mathbf{p}} = w_0\frac{12c^4 + p_{\mathrm{E}}^2(6c^2 - 11I_p) - 18c^2I_p}{3(2c^2 + p_{\mathrm{E}}^2)^2} \times\exp[-iS(p_E,\eta_s)], \tag{9}$$

where the prefactor is $w_0 \equiv 1024\pi(2I_p)^{15/2}/E(\eta_s)^2$ and $\pm$ refers to $m_j = \pm 1/2$ (in the case of the s state, the total angular moment is $J = 1/2$). The time variable is changed to the phase variable η in Eq. (2) and the η integral is calculated with the saddle-point method; η_s is the saddle-point value for the phase η [44]. There exists no asymmetry between the ionization probabilities from the spin-up and -down states $2s_+$ ($m_j = 1/2$) and $2s_-$ ($m_j = -1/2$), i.e., the ionization probabilities are equal.

For an intuitive understanding of the ionization spin asymmetry let us estimate the tunneling ionization probability via the WKB tunneling exponent

$$\Gamma \sim \exp\left(-2\left|\int_0^{r_E^{(e)}} p_E dr_E\right|\right), \tag{10}$$

where r_E is the coordinate projection along the laser electric field and $r_E^{(e)}$ is the tunnel exit coordinate. The electron momentum during the under-the-barrier-motion is complex and is derived from the energy conservation in the quasistatic tunneling picture:

$$p_E^2/2 + r_E E + \varepsilon_J^{(c)} = -I_p + \varepsilon_J^{(b)}, \tag{11}$$

where the left-hand side of the equation is the energy of the electron in the continuum during the tunneling and the right-hand side is the energy in the bound state, with the Zeeman energy splitting in the continuum $\varepsilon_J^{(c)}$ and in the bound state $\varepsilon_J^{(b)}$, respectively. From Eq. (11) $p_E = i\sqrt{2(\tilde{\epsilon} + r_E E)}$, where $\tilde{\epsilon} = I_p - \Delta\varepsilon_J$ is the effective energy during tunneling including the angular momentum–magnetic-field coupling, with $\Delta\varepsilon_J = \varepsilon_J^{(b)} - \varepsilon_J^{(c)}$. In the case of ionization from an s state the Zeeman splitting has the same magnitude in the bound state and during tunneling $\varepsilon_J^{(b)} = \varepsilon_J^{(c)} = g_S\mathbf{S}\cdot\mathbf{B}/2c$. Therefore, the electron effective energy during the tunneling does not depend on the spin projection and, consequently, the tunneling probability is the same for both states $m_j = \pm 1/2$, explaining that there is no spin asymmetry in this case.

For the p states the total angular momentum can be $J = 1/2$ or $3/2$. The wave function for the initial free bound state with $J = 1/2$ reads [45]

$$\psi_{1/2+}^{(2p)}(\mathbf{r}) = \left\{-\frac{z}{r}, -\frac{x+iy}{r}, -\frac{i(\sqrt{2I_p}r - 3)}{2cr}, 0\right\} \times\frac{(2I_p)^{5/4}re^{-\sqrt{2I_p}r}}{\sqrt{3\pi}},$$

$$\psi_{1/2-}^{(2p)}(\mathbf{r}) = \left\{\frac{x-iy}{r}, -\frac{z}{r}, 0, \frac{i(\sqrt{2I_p}r - 3)}{2cr}\right\} \times\frac{(2I_p)^{5/4}re^{-\sqrt{2I_p}r}}{\sqrt{3\pi}}.$$

They can be approximated analogously to the $2s$ states, yielding

$$\psi^{(2p)}_{1/2+}(\mathbf{r}) = \left\{-\frac{z}{r}, -\frac{x+iy}{r}, -\frac{i\sqrt{I_p}}{\sqrt{2}c}, 0\right\}\frac{(2I_p)^{5/4} r e^{-\sqrt{2I_p}r}}{\sqrt{3\pi}}, \tag{12}$$

$$\psi^{(2p)}_{1/2-}(\mathbf{r}) = \left\{\frac{x-iy}{r}, -\frac{z}{r}, 0, \frac{i\sqrt{I_p}}{\sqrt{2}c}\right\}\frac{(2I_p)^{5/4} r e^{-\sqrt{2I_p}r}}{\sqrt{3\pi}}. \tag{13}$$

As can be seen from the wave function above, they are either a linear combination of $m_l = 0, m_s = 1/2$ and $m_l = 1$, $m_s = -1/2$ or $m_l = -1, m_s = 1/2$ and $m_l = 0, m_s = -1/2$ with equal weighting, where m_l, m_s are the quantum numbers for the orbital moment and spin projections. The initial states in the SFA amplitude, which are the eigenstates of the dressed atomic Hamiltonian of Eq. (4), equal

$$\tilde{\psi}^{(2p)}_{1/2\pm} = \psi^{(2p)}_{1/2\pm}\exp(\pm iA/6c). \tag{14}$$

The Zeeman energy splitting

$$\varepsilon^{(b)}_J = g_J \mathbf{J}\cdot\mathbf{B}/2c \tag{15}$$

is determined by the Landé factor

$$g_J = \frac{3}{2} + \frac{S(S+1) - L(L+1)}{2J(J+1)}, \tag{16}$$

with $S = 1/2$, $L = 1$, and $J = 1/2$ and then $g_J = 2/3$.

In the case of the p states with $J = 3/2$, we approximate similarly the exact wave function with $m_j = 3/2$ as

$$\psi^{(2p)}_{3/2++}(\mathbf{r}) = \frac{(2I_p)^{5/4} r e^{-\sqrt{2I_p}r}}{\sqrt{2\pi}}\left\{\frac{(x+iy)}{r}, 0, \frac{i\sqrt{2I_p}z(x+iy)}{2cr^2}, \frac{i\sqrt{2I_p}(x+iy)^2}{2cr^2}\right\}, \tag{17}$$

which is a state with $m_l = 1, m_s = 1/2$. The state with $m_j = 1/2$ is approximated as

$$\psi^{(2p)}_{3/2+}(\mathbf{r}) = \frac{(2I_p)^{5/4} r e^{-\sqrt{2I_p}r}}{\sqrt{6\pi}}\left\{\frac{2z}{r}, -\frac{x+iy}{r}, \frac{i\sqrt{2I_p}(6z^2/r^2-2)}{4c}, \frac{3i\sqrt{2I_p}z(x+iy)}{2cr^2}\right\}, \tag{18}$$

which is a linear combination of $m_l = 0, m_s = 1/2$ and $m_l = 1, m_s = -1/2$ in the ratio 2:1. The state with $m_j = -1/2$ is

$$\psi^{(2p)}_{3/2-}(\mathbf{r}) = \frac{(2I_p)^{5/4} r e^{-\sqrt{2I_p}r}}{\sqrt{6\pi}}\left\{-\frac{x-iy}{r}, -\frac{2z}{r}, -\frac{3i\sqrt{2I_p}z(x-iy)}{2cr^2}, \frac{i\sqrt{2I_p}(6z^2/r^2-2)}{4c}\right\}, \tag{19}$$

which is a linear combination of $m_l = 0, m_s = -1/2$ and $m_l = -1, m_s = 1/2$ in the ratio 2:1. Finally, the state with $m_j = -3/2$ reads

$$\psi^{(2p)}_{3/2--}(\mathbf{r}) = \frac{(2I_p)^{5/4} r e^{-\sqrt{2I_p}r}}{\sqrt{2\pi}}\left\{0, \frac{(x-iy)}{r}, \frac{i\sqrt{2I_p}(x-iy)^2}{2cr^2}, -\frac{i\sqrt{2I_p}z(x-iy)}{2cr^2}\right\}, \tag{20}$$

which is a state with $m_l = -1, m_s = -1/2$. The dressed states in the SFA amplitude are calculated

$$\tilde{\psi}^{(2p)}_{3/2\pm\pm} = \psi^{(2p)}_{3/2\pm\pm}\exp(\pm iA/c),$$
$$\tilde{\psi}^{(2p)}_{3/2\pm} = \psi^{(2p)}_{3/2\pm}\exp(\pm iA/3c). \tag{21}$$

Again with the help of the Landé factor the Zeeman energy splitting can be given, with $S = 1/2$, $J = 3/2$, $L = 1$, and $g_J = 4/3$ in this case.

In following sections we consider three physically relevant possible choices of the quantization axis for the angular momentum and spin: (a) along the laser magnetic-field direction, (b) along the laser propagation direction, and (c) along the electric-field direction.

III. QUANTIZATION AXIS ALONG THE LASER MAGNETIC-FIELD DIRECTION

When the quantization axis is along the laser magnetic-field direction, no spin flip can occur during ionization. Let us first consider the case of $J = 1/2$. We calculate the probability for the ionization from a p state ($J = 1/2$) with the total angular momentum projection $m_j = \pm 1/2$. The corresponding relative differential probabilities with respect to the $2s$ state on the momentum parabola of Eq. (8) are

$$\frac{dw^{(2p)}_{1/2\pm}/d^3\mathbf{p}}{dw^{(2s)}/d^3\mathbf{p}} = \frac{w^{(2p)}_{1/2\pm}}{w^{(2s)}} = \frac{1}{3} \pm \frac{2\sqrt{2I_p/c^2}}{9}, \tag{22}$$

where I_p/c^2 terms are neglected. The latter is illustrated in Fig. 1. There is a nonvanishing spin asymmetry with respect to tunneling ionization

$$\mathcal{A}^{(2p)}_{1/2} = \left|\frac{dw^{(2p)}_{1/2+}/d^3\mathbf{p} - dw^{(2p)}_{1/2-}/d^3\mathbf{p}}{dw^{(2p)}_{1/2+}/d^3\mathbf{p} + dw^{(2p)}_{1/2-}/d^3\mathbf{p}}\right| \approx \frac{2}{3}\left(\frac{2I_p}{c^2}\right)^{1/2}. \tag{23}$$

Intuitively one can understand the ionization asymmetry between $2p_{1/2+}$ and $2p_{1/2-}$ states (the splitting of the middle line in Fig. 1) in the following way. In the nonrelativistic limit at this choice of the quantization axis, predominantly the states with $m_l = \pm 1$ are ionized (this corresponds to $m_l = 0$ for the more usual choice of the quantization axis along the electric field). The state with $m_j = 1/2$ is a linear combination of $m_l = 0, m_s = 1/2$ and $m_l = 1, m_s = -1/2$ states, from which only the part of the bound-state wave function with $m_l = 1$ can be ionized, which has here a weight of 1/2. Accordingly,

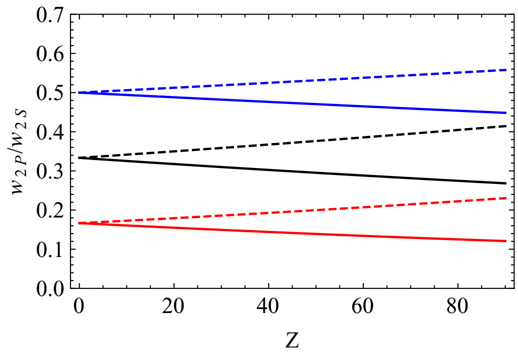

FIG. 1. (Color online) Relative and total ionization rates of the $2p$ states $dw^{(2p)}/d^3\mathbf{p}$ with respect to the $2s$ state $dw^{(2s)}/d^3\mathbf{p}$ vs the hydrogenlike ion charge Z, when the angular momentum quantization axis is along the laser magnetic field: blue (top) lines, $2p_{3/2++}\to\uparrow$ (dashed) and $2p_{3/2,--}\to\downarrow$ (solid); red (bottom) lines, $2p_{3/2+}\to\downarrow$ (dashed) and $2p_{3/2-}\to\uparrow$ (solid); black (middle) lines, $2p_{1/2+}\to\downarrow$ (dashed) and $2p_{1/2-}\to\uparrow$ (solid). The final electron spin is indicated by $\uparrow$ or $\downarrow$; the subscript $\pm\pm$ indicates $m_j=\pm 3/2$ and $\pm$ indicates $m_j=\pm 1/2$.

the state with $m_j=-1/2$ is the linear combination of $m_l=0$, $m_s=-1/2$ and $m_l=-1, m_s=1/2$ states, from which only the part with $m_l=-1$ can be ionized. Therefore, the spin of the tunneling electron in the states $m_j=\pm 1/2$ are opposite $m_s=\mp 1/2$. We can estimate the tunneling ionization probability via the WKB tunneling exponent (10),

$$\Gamma^{(2p)}_{1/2\pm}\sim\exp\left(-\frac{4\sqrt{2}}{3}\frac{\tilde{\epsilon}^{3/2}}{E_0}\right)\approx e^{-(2/3)(E_a/E_0)}\left(1+\frac{\Delta\varepsilon_J E_a}{I_p E_0}\right), \tag{24}$$

where $\Delta\varepsilon_J=g_J\mathbf{J}\cdot\mathbf{B}/2c-g_S\mathbf{S}\cdot\mathbf{B}/2c$ as the Zeeman energy splitting in the bound state is $\varepsilon_J^{(b)}=g_J\mathbf{J}\cdot\mathbf{B}/2c$, whereas during tunneling it is $\varepsilon_J^{(c)}=g_S\mathbf{S}\cdot\mathbf{B}/2c$. Then $\Delta\varepsilon_J=2E_0/3c$ and, according to Eq. (24),

$$\Gamma^{(2p)}_{1/2\pm}\sim e^{-(2/3)(E_a/E_0)}\left[1\pm\frac{4}{3}\left(\frac{2I_p}{c^2}\right)^{1/2}\right], \tag{25}$$

when $J=\pm 1/2$ and $S=\mp 1/2$.

Further, there is a second reason for the asymmetry in the ionization probability. In a p state the electron rotates around the atomic core in the k-E plane at $m_l=\pm 1$ (the quantization axis is along the magnetic field). Since there is a shift due to the laser magnetic field in the k direction [6,7], it matters if the rotation is parallel or antiparallel to the shift during tunneling that disturbs the ionization probability. Mathematically, the bound-state wave function has the form $\psi^{(2p)}_{1/2\pm}(\mathbf{p},t_s)\sim 1\mp ip_{k,s}/p_{E,s}$ at the saddle point, i.e., at the moment when ionization starts. With $p_{ks}=-2I_p/3c$ and $p_E=-i\sqrt{2I_p}$ it follows that

$$\left|\psi^{(2p)}_{1/2\pm}(\mathbf{p},t_s)\right|^2\sim 1\mp\frac{2}{3}\left(\frac{2I_p}{c^2}\right)^{1/2}. \tag{26}$$

Therefore, the ionization is preferable from the state where in the bound state the electron rotation is opposite to the rotation of the electron due to the Lorentz force. (A similar effect exists in the nonadiabatic tunneling in a circularly polarized laser field [38], when the ionization is preferable from the state where in the bound state the electron rotation is opposite to the rotation of the field.) Adding these two effects—the different angular momentum–magnetic-field coupling in the bound state and during tunneling and momentum selective tunneling from a p state—the calculated asymmetries of Eq. (23) are explained.

The asymmetries for $2p_{3/2}$ states have the same origin. The derived respective ionization rates are (see Fig. 1)

$$\frac{dw^{(2p)}_{3/2\pm\pm}/d^3\mathbf{p}}{dw^{(2s)}/d^3\mathbf{p}}=\frac{w^{(2p)}_{3/2\pm\pm}}{w^{(2s)}}=\frac{1}{2}\pm\frac{(2I_p/c^2)^{1/2}}{6}, \tag{27}$$

$$\frac{dw^{(2p)}_{3/2\pm}/d^3\mathbf{p}}{dw^{(2s)}/d^3\mathbf{p}}=\frac{w^{(2p)}_{3/2\pm}}{w^{(2s)}}=\frac{1}{6}\pm\frac{(2I_p/c^2)^{1/2}}{6} \tag{28}$$

(I_p/c^2 terms are neglected), which yields the asymmetries

$$\mathcal{A}^{(2p)}_{3/2,3/2}=\left|\frac{dw^{(2p)}_{3/2++}/d^3\mathbf{p}-dw^{(2p)}_{3/2--}/d^3\mathbf{p}}{dw^{(2p)}_{3/2++}/d^3\mathbf{p}+dw^{(2p)}_{3/2--}/d^3\mathbf{p}}\right|\approx\frac{1}{3}\left(\frac{2I_p}{c^2}\right)^{1/2}, \tag{29}$$

$$\mathcal{A}^{(2p)}_{3/2,1/2}=\left|\frac{dw^{(2p)}_{3/2+}/d^3\mathbf{p}-dw^{(2p)}_{3/2-}/d^3\mathbf{p}}{dw^{(2p)}_{3/2+}/d^3\mathbf{p}+dw^{(2p)}_{3/2-}/d^3\mathbf{p}}\right|\approx\left(\frac{2I_p}{c^2}\right)^{1/2}, \tag{30}$$

Here again only parts of the bound-state wave function are allowed to tunnel that have quantum number $m_l=\pm 1$. The $2p_{3/2++}$ state is represented via the state with $m_l=1$, $m_s=1/2$, while the $2p_{3/2--}$ state is represented via $m_l=-1$, $m_s=-1/2$ (spins are opposite). Then, according to Eq. (24),

$$\Gamma^{(2p)}_{3/2\pm\pm}\sim e^{-(2/3)(E_a/E_0)}\left[1\pm\left(\frac{2I_p}{c^2}\right)^{1/2}\right], \tag{31}$$

when $J=\pm 3/2$ and $S=\pm 1/2$, while the asymmetry due to the electron rotation in the bound state is the same as in the $J=1/2$ case,

$$\left|\psi^{(2p)}_{3/2\pm\pm}(\mathbf{p},t_s)\right|^2\sim 1\mp\frac{2}{3}\left(\frac{2I_p}{c^2}\right)^{1/2}, \tag{32}$$

leading finally to Eq. (29). Similarly, the $2p_{3/2+}$ state in the ionization contributes $m_l=1, m_s=-1/2$ state and the $2p_{3/2-}$ state contributes $m_l=-1, m_s=1/2$ and

$$\Gamma^{(2p)}_{3/2\pm}\sim e^{-(2/3)(E_a/E_0)}\left[1\pm\frac{5}{3}\left(\frac{2I_p}{c^2}\right)^{1/2}\right], \tag{33}$$

which again leads to Eq. (30), taking into account Eq. (32).

Thus, the asymmetry of ionization from a p state, which is expressed by the splitting of the curves in Fig. 1, is due to the difference of the angular momentum coupling with the laser magnetic field in the bound state and during tunneling as well as to the fact that the ionization is larger from that bound state where the electron rotation is opposite to the electron relativistic shift along the propagation direction. However, the first effect dominates. The values of the ionization probability at $Z\to 0$ in Fig. 1 can be easily deduced, taking into account the nonrelativistic relation between ionization probabilities of the s and p states (mostly $m_l=\pm 1$ states contribute to ionization) as well as the fact that the relative weight of the $m_l = 1$ state in the states $2p_{3/2,3/2}$, $2p_{1/2,1/2}$, and $2p_{3/2,1/2}$ are 3/2:1:1/2, which follows from the expression of the corresponding wave functions from Eqs. (12)–(20).

IV. QUANTIZATION AXIS ALONG THE LASER PROPAGATION DIRECTION

Now let us consider the choice of the quantization axis along the laser propagation direction. In this case the angular momentum and the spin of the active electron is not constant before the tunneling starts, in contrast to the previous case of the quantization axis along the magnetic field and the process is altered. In particular, the spin flip becomes possible. Further, nonrelativistically again, only $m_l = \pm 1$ components of the bound-state wave function are allowed to tunnel. The results for the total ionization probability of the $2p_{1/2}$ states are (see Fig. 2)

$$\frac{w^{(2p)}_{1/2+}}{w^{(2s)}} \approx \frac{w^{(2p)}_{1/2-}}{w^{(2s)}} \approx \frac{1}{3}, \tag{34}$$

where the relatively unimportant I_p/c^2 terms are dropped. The ionization probabilities are almost constant, which is easy to understand as follows. The states with angular momentum up or down evolve in the bound state and mix. They can be represented by another basis where the angular momentum is aligned along the laser magnetic field and are a linear superposition of these states. Since the ionization probabilities of these new basis states are in the leading order the same as shown in the previous section [see Eq. (22)], also every superposition has the same ionization probability, which explains our observation.

For the $2p_{3/2}$ states the relative ionization probabilities are (see Fig. 2)

$$\frac{w^{(2p)}_{3/2\pm\pm}}{w^{(2s)}} = \frac{1}{4} + \frac{1}{4}\exp\left(-\frac{4\mu^2}{3}\right), \tag{35}$$

$$\frac{w^{(2p)}_{3/2\pm}}{w^{(2s)}} = \frac{5}{12} - \frac{1}{4}\exp\left(-\frac{4\mu^2}{3}\right), \tag{36}$$

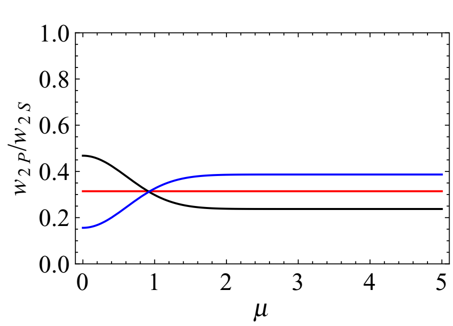

FIG. 2. (Color online) Relative ionization rates of $2p$ states $dw^{(2p)}/d^3\mathbf{p}$ with respect to the $2S$ state $dw^{(2s)}/d^3\mathbf{p}$ vs the laser intensity parameter $\mu = \sqrt{E_0/E_a}E_0/c\omega$, when the angular momentum quantization axis is along the laser propagation: black (top) line at $\mu \to 0$, $P_{3/2,++} \to\uparrow/\downarrow$; blue (bottom) line at $\mu \to 0$, $P_{3/2,+} \to\uparrow/\downarrow$; and red (middle) line at $\mu \to 0$, $P_{1/2,+} \to\uparrow/\downarrow$. The summation over the electron final spin is indicated by $\uparrow/\downarrow$; the subscript $++$ indicates $m_j = 3/2$ and $+$ indicates $m_j = 1/2$.

where $\mu = \sqrt{E_0/E_a}E_0/c\omega$ is the strong-field parameter for the spin-flip effects (see Ref. [20]). Here also the relatively unimportant I_p/c^2 dependence was dropped.

One can see that the ionization probabilities for the $2p_{3/2}$ states change significantly when entering the strong-field regime when $\mu \gtrsim 1$ (see Fig. 2). Note that $\mu \sim 1$ can be achieved using highly charged ions with a charge $Z \sim 20$ in a laser field with intensity 10^{21} W/cm^2. For an explanation we express the evolving states via the basis where the angular momentum is aligned along the magnetic field. Now the states of this basis have different ionization probabilities [see Eq. (27)] and the total ionization probability depends on the particular superposition of these states. Moreover, the superposition depends on the bound dynamics, which is different for different μ, i.e., for different laser-field strengths [see Eq. (21)].

For instance, the state $2p_{3/2++}$ can be expressed in the basis with the quantization axis along magnetic field as

$$|3/2++\rangle_k = \alpha_1|3/2++\rangle_B + \alpha_2|3/2+\rangle_B + \alpha_3|3/2-\rangle_B + \alpha_4|3/2--\rangle_B, \tag{37}$$

with $\alpha_1 = 1/(2\sqrt{2})\exp(iA/c)$, $\alpha_2 = \sqrt{3}/(2\sqrt{2})\exp(iA/6c)$, $\alpha_3=\sqrt{3}/(2\sqrt{2})\exp(-iA/6c)$, and $\alpha_4=1/(2\sqrt{2})\exp(-iA/c)$. The states $|3/2++\rangle_B$ and $|3/2+\rangle_B$ have different ionization probabilities, the ratio of the probabilities is $W^{(2p)}_{3/2++;B}$:$W^{(2p)}_{3/2+;B} = 1/2$:$1/6$ [see Eq. (27)], and the field-dependent phases due to Zeeman splitting are different as well. Therefore, the ionization probability is essentially field dependent.

Whereas for small field strength the phases are negligible $A/c \ll 1$ ($\mu \ll 1$), for large field strength they average out. Because of that, at $\mu \gg 1$ the total ionization rate of the $|3/2++\rangle_k$ state can be given by

$$W^{(2p)}_{3/2++} \approx \sum_{i=1}^{4} |\alpha_i|^2|M_i|^2 = \frac{1}{4}, \tag{38}$$

with $|M_1|^2 \approx |M_4|^2 = W^{(2p)}_{3/2++;B} = 1/2$ and $|M_2|^2 \approx |M_3|^2 = W^{(2p)}_{3/2+;B} = 1/6$, explaining the $\mu \gg 1$ asymptotic behavior of the black line in Fig. 2. The $\mu \gg 1$ asymptotics of the other curves can be explained similarly.

In the weak-field limit $\mu \ll 1$ the phases $\sim A/c$ determining the angular momentum precession in the magnetic field can be neglected. In this case the total ionization rate for the $|3/2++\rangle_k$ state can be given by

$$W^{(2p)}_{3/2++} \approx |\alpha_1 M_1 + \alpha_3 M_3|^2 + |\alpha_2 M_2 + \alpha_4 M_4|^2 \tag{39}$$

$$\approx \left|\tfrac{1}{4} + \tfrac{1}{4}\right|^2 + \left|\tfrac{1}{4} + \tfrac{1}{4}\right|^2 = \tfrac{1}{2}. \tag{40}$$

which explains the $\mu \ll 1$ asymptotics of the black line in Fig. 2. Here we note that the states $|Jm_j\rangle_B$ do not precess in the laser field and ionize into states with spin up with respect to the magnetic field when $m_j = 3/2$ or $m_j = -1/2$ or spin down in the case $m_j = 1/2$ or $m_j = -3/2$, respectively. That is why in Eq. (40) M_1 interferes only with M_3 and M_2 interferes only with M_4.

Thus, in weak laser fields there is interference in the ionization probability from the superposition of states, while

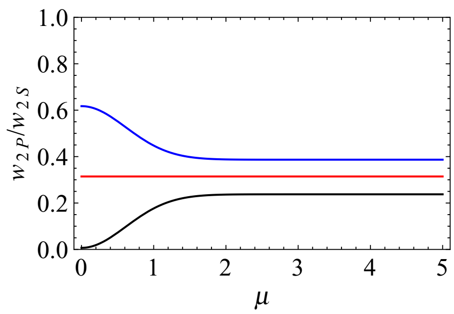

FIG. 3. (Color online) Relative ionization rates of $2p$ states $dw^{(2p)}/d^3\mathbf{p}$ with respect to the $2S$ state $dw^{(2s)}/d^3\mathbf{p}$ vs the laser intensity parameter $\mu = \sqrt{E_0/E_a}E_0/c\omega$, when the angular momentum quantization axis is along the laser electric-field direction: black (bottom) line, $P_{3/2++} \to \uparrow/\downarrow$; blue (top) line, $P_{3/2+} \to \uparrow/\downarrow$; and red (middle) line, $P_{1/2,+} \to \uparrow/\downarrow$. The summation over the electron final spin is indicated by $\uparrow/\downarrow$; the subscript $++$ indicates $m_j = 3/2$ and $+$ indicates $m_j = 1/2$.

in strong fields the interference is wiped out because of the fast precession of the bound state. This has the consequence that the m_j dependence of the ionization rate is different in weak- and strong-field asymptotics (see Fig. 2).

V. QUANTIZATION AXIS ALONG THE LASER ELECTRIC FIELD

Finally, let us consider the case when the quantization axis is along the laser electric field. Here, nonrelativistically, parts of the bound-state wave function with quantum number $m_l = 0$ are allowed to tunnel through the barrier. Therefore, the $2p_{3/2++}$ and $2p_{3/2--}$ states have zero ionization probability for weak laser fields (see Fig. 3).

For the $2p_{3/2}$ states the relative ionization probabilities are (see Fig. 3)

$$\frac{w^{(2p)}_{3/2\pm\pm}}{w^{(2s)}} \approx \frac{1}{4} - \frac{1}{4}\exp\left(-\frac{4\mu^2}{3}\right), \tag{41}$$

$$\frac{w^{(2p)}_{3/2\pm}}{w^{(2s)}} \approx \frac{5}{12} + \frac{1}{4}\exp\left(-\frac{4\mu^2}{3}\right), \tag{42}$$

where again I_p/c^2 corrections are dropped. The intuitive explanation of the asymptotic behavior of the ionization probabilities for small and large laser-field strength can be done analogous to that of the previous section.

VI. CONCLUSION

We have investigated the tunneling ionization of a highly charged ion from an excited p state of a hydrogenlike ion in a linearly polarized strong laser field in the relativistic regime. The ionization picture is analyzed in three possible setups for the angular momentum and spin quantization axis. When the quantization axis is along the laser magnetic field, then there is no spin-flip effect but there is a large spin asymmetry. This is in contrast to the case of the ionization from an s state where the spin asymmetry is vanishing. The spin asymmetry of the p-state ionization is due to two reasons. First, there is a difference in the Zeeman splitting of the electron energy in the bound state and during tunneling. Second, in the relativistic regime the tunneling electron acquires a shift along the laser propagation direction during the under-the-barrier motion due to the $\mathbf{v} \times \mathbf{B}$ force. The ionization probability is larger for those states (for such a magnetic quantum number) where the electron rotation in the bound state in the $(\mathbf{k},\mathbf{E})$ plane is opposite to the relativistic shift. Because at a certain value of the projection of the total angular momentum the spin states are entangled with the states of the magnetic quantum number, the mentioned asymmetry with respect to the magnetic quantum number is observed as a spin asymmetry.

In the case when the spin quantization axis is along the laser propagation direction (or along the laser electric field), we have investigated the dependence of the ionization rate on the laser intensity for different projections of the total angular momentum m_j. The dependence of the ionization rate on the projection of the total angular momentum appears to be different for weak and strong fields (nonrelativistic and relativistic regimes). Moreover, the m_j dependence of the ionization rate in the relativistic regime is reverted with respect to the case of the nonrelativistic regime. We have identified the intensity parameter $\mu = \sqrt{E_0/E_a}(E_0/c\omega)$, which governs this behavior. Correspondingly, the intensity dependence of the ionization rate is different for the states with different projections of the total angular momentum. This effect can be observed using highly charged ions with a charge $Z \sim 20$ in a laser field with intensity 10^{21} W/cm^2. We have provided an intuitive description of these properties. The state with a certain total angular momentum along the laser propagation (field) direction can be represented as a superposition of states with different projections of the total angular momentum on the magnetic-field direction. In weak laser fields there is interference in the ionization probability from the above-mentioned superposition of states. Meanwhile, in strong fields the fast precession of the bound state destroys the interference in ionization.

ACKNOWLEDGMENTS

We gratefully acknowledge helpful discussions with Professor C. H. Keitel. K.Z.H. acknowledges that this research was supported in part by the National Science Foundation (USA) under Grant No. NSF PHY11-25915.

[1] A. D. DiChiara, I. Ghebregziabher, R. Sauer, J. Waesche, S. Palaniyappan, B. L. Wen, and B. C. Walker, Phys. Rev. Lett. **101**, 173002 (2008).

[2] S. Palaniyappan, R. Mitchell, R. Sauer, I. Ghebregziabher, S. L. White, M. F. Decamp, and B. C. Walker, Phys. Rev. Lett. **100**, 183001 (2008).

[3] A. D. DiChiara, I. Ghebregziabher, J. M. Waesche, T. Stanev, N. Ekanayake, L. R. Barclay, S. J. Wells, A. Watts, M. Videtto, C. A. Mancuso, and B. C. Walker, Phys. Rev. A **81**, 043417 (2010).

[4] N. Ekanayake, S. Luo, P. D. Grugan, W. B. Crosby, A. D. Camilo, C. V. McCowan, R. Scalzi, A. Tramontozzi, L. E. Howard, S. J. Wells, C. Mancuso, T. Stanev, M. F. Decamp, and B. C. Walker, Phys. Rev. Lett. **110**, 203003 (2013).

[5] A. Di Piazza, C. Müller, K. Z. Hatsagortsyan, and C. H. Keitel, Rev. Mod. Phys. **84**, 1177 (2012).

[6] M. Klaiber, E. Yakaboylu, H. Bauke, K. Z. Hatsagortsyan, and C. H. Keitel, Phys. Rev. Lett. **110**, 153004 (2013).

[7] E. Yakaboylu, M. Klaiber, H. Bauke, K. Z. Hatsagortsyan, and C. H. Keitel, Phys. Rev. A **88**, 063421 (2013).

[8] E. Yakaboylu, M. Klaiber, and K. Z. Hatsagortsyan, Phys. Rev. A **90**, 012116 (2014).

[9] S. Ahrens, H. Bauke, C. H. Keitel, and C. Müller, Phys. Rev. Lett. **109**, 043601 (2012).

[10] S. Ahrens, H. Bauke, C. H. Keitel, and C. Müller, Phys. Rev. A **88**, 012115 (2013).

[11] O. D. Skoromnik, I. D. Feranchuk, and C. H. Keitel, Phys. Rev. A **87**, 052107 (2013).

[12] M. Wen, H. Bauke, and C. H. Keitel, arXiv:1406.3659.

[13] H. Bauke, S. Ahrens, C. H. Keitel, and R. Grobe, New J. Phys. **16**, 103028 (2014).

[14] H. Bauke, S. Ahrens, C. H. Keitel, and R. Grobe, Phys. Rev. A **89**, 052101 (2014).

[15] H. Bauke, S. Ahrens, C. H. Keitel, and R. Grobe, New J. Phys. **16**, 043012 (2014).

[16] M. W. Walser, D. J. Urbach, K. Z. Hatsagortsyan, S. X. Hu, and C. H. Keitel, Phys. Rev. A **65**, 043410 (2002).

[17] S. X. Hu and C. H. Keitel, Phys. Rev. Lett. **83**, 4709 (1999).

[18] M. W. Walser and C. H. Keitel, Opt. Commun. **199**, 447 (2001).

[19] F. H. M. Faisal and S. Bhattacharyya, Phys. Rev. Lett. **93**, 053002 (2004).

[20] M. Klaiber, E. Yakaboylu, C. Müller, H. Bauke, G. G. Paulus, and K. Z. Hatsagortsyan, J. Phys. B **47**, 065603 (2014).

[21] S. Bhattacharyya, M. M., J. Chakrabarti, and F. H. M. Faisal, J. Phys. Conf. Ser. **80**, 012029 (2007).

[22] S. Bhattacharyya, M. Mazumder, J. Chakrabarti, and F. H. M. Faisal, Phys. Rev. A **83**, 043407 (2011).

[23] A. M. Perelomov and V. S. Popov, Zh. Eksp. Teor. Fiz. **50**, 1393 (1966).

[24] A. M. Perelomov, V. S. Popov, and V. M. Terent'ev, Zh. Eksp. Teor. Fiz. **51**, 309 (1966) [Sov. Phys. JETP **23**, 924 (1966)].

[25] A. M. Perelomov and V. S. Popov, Zh. Eksp. Teor. Fiz. **52**, 514 (1967) [Sov. Phys. JETP **25**, 336 (1967)].

[26] M. V. Ammosov, N. B. Delone, and V. P. Krainov, Zh. Eksp. Teor. Fiz. **91**, 2008 (1986) [Sov. Phys. JETP **64**, 1191 (1986)].

[27] V. S. Popov, B. M. Karnakov, and V. D. Mur, Pis'ma Zh. Eksp. Teor. Fiz. **79**, 320 (2004) [JETP Lett. **79**, 262 (2004)].

[28] B. A. Zon and A. S. Kornev, J. Eksp. Teor. Phys. **101**, 1009 (2005).

[29] C. Liu and M. Nisoli, Phys. Rev. A **85**, 013418 (2012).

[30] M. Lein, J. Phys. B **36**, L155 (2003).

[31] T. K. Kjeldsen, C. Z. Bisgaard, L. B. Madsen, and H. Stapelfeldt, Phys. Rev. A **68**, 063407 (2003).

[32] R. Fischer, M. Lein, and C. H. Keitel, Phys. Rev. Lett. **97**, 143901 (2006).

[33] S. J. McNaught, J. P. Knauer, and D. D. Meyerhofer, Phys. Rev. Lett. **78**, 626 (1997).

[34] C. I. Moore, A. Ting, S. J. McNaught, J. Qiu, H. R. Burris, and P. Sprangle, Phys. Rev. Lett. **82**, 1688 (1999).

[35] K. Yamakawa, Y. Akahane, Y. Fukuda, M. Aoyama, N. Inoue, H. Ueda, and T. Utsumi, Phys. Rev. Lett. **92**, 123001 (2004).

[36] E. Gubbini, U. Eichmann, M. Kalashnikov, and W. Sandner, Phys. Rev. Lett. **94**, 053602 (2005).

[37] R. Taïeb, V. Véniard, and A. Maquet, Phys. Rev. Lett. **87**, 053002 (2001).

[38] I. Barth and O. Smirnova, Phys. Rev. A **84**, 063415 (2011).

[39] I. Barth and O. Smirnova, Phys. Rev. A **87**, 013433 (2013).

[40] T. Herath, L. Yan, S. K. Lee, and W. Li, Phys. Rev. Lett. **109**, 043004 (2012).

[41] L. V. Keldysh, Zh. Eksp. Teor. Fiz. **47**, 1945 (1964) [Sov. Phys. JETP **20**, 1307 (1965)].

[42] I. Barth and O. Smirnova, Phys. Rev. A **88**, 013401 (2013).

[43] M. Klaiber, E. Yakaboylu, and K. Z. Hatsagortsyan, Phys. Rev. A **87**, 023417 (2013).

[44] M. Klaiber, E. Yakaboylu, and K. Z. Hatsagortsyan, Phys. Rev. A **87**, 023418 (2013).

[45] H. A. Bethe and E. E. Salpeter, *Quantum Mechanics of One- and Two-Electron Atoms* (Academic, New York, 1957).